Electronic structure of self-assembled InAs quantum discs in a magnetic field with varying orientation and two-electron quantum-disc qubits

2005 J. Phys.: Condens. Matter 17 949

(http://iopscience.iop.org/0953-8984/17/6/012)

INSTITUTE OF PHYSICS PUBLISHING JOURNAL OF PHYSICS: CONDENSED MATTER

J. Phys.: Condens. Matter **17** (2005) 949–955 doi:10.1088/0953-8984/17/6/012

Electronic structure of self-assembled InAs quantum discs in a magnetic field with varying orientation and two-electron quantum-disc qubits

Qing-Rui Dong, Shu-Shen Li, Zhi-Chuan Niu and Song-Lin Feng

State Key Laboratory for Superlattices and Microstructures, Institute of Semiconductors, Chinese Academy of Sciences, PO Box 912, Beijing 100083, People's Republic of China

Received 9 November 2004, in final form 4 January 2005
Published 28 January 2005
Online at stacks.iop.org/JPhysCM/17/949

Abstract

We have studied the electronic structure of vertically assembled quantum discs in a magnetic field with varying orientation using the effective mass approximation. We calculate the four energy levels of single-electron quantum discs and the two lowest energy levels of two-electron quantum discs in a magnetic field with varying orientation. The change of the magnetic field as an effective potential strongly modifies the electronic structure, leading to splittings of the levels and anticrossings between the levels. The calculated results also demonstrate the switching between the ground states with the total spin $S = 0$ and 1. The switching induces a qubit controlled by varying the orientation of the magnetic field.

1. Introduction

A semiconductor quantum dot (QD) is physically similar to a set of atomic electrons bound to a nucleus and, for this reason, these structures are sometime termed 'artificial atoms'. To extend the atomic analogy further, QDs are considered as 'artificial molecules' [1] if they join together. The molecular orbitals of coupled QDs have been investigated theoretically [2–6]. In relevant calculations, Harju *et al* [6] studied a two-electron QD molecule consisting of two laterally coupled QDs in a magnetic field by the direct diagonalization of the Hamiltonian matrix and designed a qubit using the total spin of the two-electron molecule. Fonseca *et al* [5] studied stacked pyramids using an effective mass approximation with the effects of strain and piezoelectric potential as local modifications of the conduction band offset. In experimental investigations [7–9] on coupled QDs, progress in the 'indium-flush' [7] technique led to high-quality vertically stacked quantum discs. Applications of vertically aligned structures are focused on fabricating QD lasers [10, 11], light storage devices [12] and quantum computers [13–17]. Burkard *et al* [13] obtained the electronic structure and exchange coupling (the energy difference between the singlet and triplet in a coupled pair of dots) for two orientations of the magnetic field: parallel and perpendicular to the growth plane.

Pazy *et al* [14] obtained sub-picosecond spin-dependent switching of the Coulomb interaction in an array of self-assembled InAs QDs for potential application in quantum information processing. The existence of a strong built-in electric field [16] induced by the spontaneous polarization and the piezoelectricity is exploited to generate entangled few-exciton states in coupled quantum dots without resorting to external fields. Korkusiski *et al* [18] studied the energy spectrum of the structures in the adiabatic approximation and the influence of the strain and dot separation on the formation of coupled QD levels.

We concentrate our attention on vertically assembled quantum discs consisting of two coupled disc-shaped QDs. The vertically assembled structure has previously been studied in [18, 17] where the applied external magnetic field is perpendicular to and parallel to the growth direction, while in the present study we introduce the magnetic field in varying orientations as an effective potential, which generalizes the results of [13] to arbitrary orientations of the magnetic field. The change of the magnetic field strongly modifies the electronic structure, leading to splittings of the levels and anticrossings between the levels. On the basis of these results, the calculation of two-electron levels is carried out by means of direct diagonalization of the Hamiltonian matrix. Our results show that the electron correlations may lead to switching of the total spin between $S = 0$ and 1 states [6]. Unlike in [6], we realize the switching by changing the orientation of an external magnetic field. Our results support the possibility of using the total spin of the system as a qubit controlled by varying the orientation of the magnetic field. Since high-quality vertically stacked quantum discs can be fabricated successfully [7], it is realistic to envisage obtaining qubits of this type.

2. The electronic structures of single-electron quantum discs

We assume that the two disc-shaped InAs QDs are two cylinders. Each disc grows on a wetting layer (WL) of thickness W covered by a GaAs barrier. The two quantum discs have the same height H (typically 1–2 nm) and the same radius R (typically 7–12 nm). The distance between the two wetting layers, D, forms a quantum tunnelling barrier of thickness $D - H$, and the conduction band offset between the quantum discs and the surrounding material gives rise to the confining potential V_0 for the quantum discs. The material parameters of the quantum discs and WLs have their effects through the effective Rydberg $R_y = m_e e^4/2\epsilon^2\hbar^2$ and the effective Bohr radius $a_B = \epsilon\hbar^2/m_e e^2$, where m_e and ϵ are the effective mass of an electron and the dielectric constant, respectively. Throughout this paper, we use R_y and a_B as the units of energy and length, respectively.

We first investigate the electronic structure of single-electron vertically assembled quantum discs in a magnetic field with varying orientation using the effective mass approximation. If the z direction is chosen to be in the heterostructure growth direction, the external magnetic field can be expressed as $\mathbf{B} = B(0, \cos\alpha, \sin\alpha)$, α being the polar angle relative to the y axis. With the vector potential $\mathbf{A} = (Bz\cos\alpha - By\sin\alpha/2, Bx\sin\alpha/2, 0)$, the Schrödinger equation in cylindrical coordinates is written as

$$H\psi(r,\theta,z) = E\psi(r,\theta,z), \tag{1}$$

where

$$\begin{aligned} H = {} & -\frac{1}{r^2}\left(r\frac{\partial}{\partial r}r\frac{\partial}{\partial r} + \frac{\partial^2}{\partial\theta^2}\right) + \frac{\Omega\sin\alpha}{2\hbar}l_z + \frac{\Omega^2 R_y m_e \sin^2\alpha}{8\hbar}r^2 + \frac{\Omega^2 R_y z^2}{2m_e\hbar^2}\cos^2\alpha \\ & - \frac{\Omega^2 R_y z r}{2m_e\hbar^2}\sin\alpha\cos\alpha\sin\theta + \mathrm{i}\Omega z\cos\alpha\left(\frac{1}{r\sin\theta}\frac{\partial}{\partial\theta} - \frac{\partial}{\cos\theta\,\partial r}\right) \\ & - \frac{\partial^2}{\partial z^2} + V(r,z), \end{aligned} \tag{2}$$

with the potential $V(r,z) = -V_0$ inside the WL and quantum discs, and $V(r,z) = 0$ in the barrier, where $\Omega = \omega_c/R_y$, $\omega_c = \hbar eB/m_e c$. In order to solve equation (1), we divide H into

$$H^{(1)} = -\frac{1}{r^2}\left(r\frac{\partial}{\partial r}r\frac{\partial}{\partial r} + \frac{\partial^2}{\partial\theta^2}\right) + \frac{\Omega\sin\alpha}{2\hbar}l_z + \frac{\Omega^2 R_y m_e \sin^2\alpha}{8\hbar}r^2 - \frac{\partial^2}{\partial z^2} + V(r,z), \tag{3}$$

and

$$H^{(2)} = \frac{\Omega^2 R_y z^2}{2m_e\hbar^2}\cos^2\alpha - \frac{\Omega^2 R_y zr}{2m_e\hbar^2}\sin\alpha\cos\alpha\sin\theta + \mathrm{i}\Omega z\cos\alpha\left(\frac{1}{r\sin\theta}\frac{\partial}{\partial\theta} - \frac{\partial}{\cos\theta\partial r}\right). \tag{4}$$

In the following, we will obtain the eigenvectors of the Hamiltonian $H^{(1)}$. Then, using the eigenvectors as basis functions, we can obtain the Hamiltonian matrix of H. By direct diagonalization of the Hamiltonian matrix, the eigenvectors and eigenvalues of the Hamiltonian H will be obtained. In the adiabatic approximation [18], the eigenfunctions of the Hamiltonian $H^{(1)}$ are written as $(1/\sqrt{2})\mathrm{e}^{\mathrm{i}m\theta}g_r^v(z)f_m^v(r)$. The functions $g_r^v(z)$ and $f_m^v(r)$ satisfy the following set of equations [18]:

$$\left[-\frac{\partial^2}{\partial z^2} + V(r,z)\right]g_r^v(z) = E_v(r)g_r^v(z), \tag{5}$$

$$[H_R + E_v(r)]f_m^v(r) = Ef_m^v(r). \tag{6}$$

$$H_R = -\frac{1}{r^2}\left(r\frac{\partial}{\partial r}r\frac{\partial}{\partial r} + \frac{\partial^2}{\partial\theta^2}\right) + \frac{\Omega\sin\alpha}{2\hbar}l_z + \frac{\Omega^2 R_y m_e\sin^2\alpha}{8\hbar}r^2. \tag{7}$$

By using the transfer matrix formalism, the eigenfunctions of the Hamiltonian $H^{(1)}$, $(1/\sqrt{2})\mathrm{e}^{\mathrm{i}m\theta}g_r^v(z)f_m^v(r)$, are obtained. Details of the computational procedure can be found elsewhere [17]. Using $(1/\sqrt{2})\mathrm{e}^{\mathrm{i}m\theta}g_r^v(z)f_m^v(r)$ as the basis function, we rewrite the Hamiltonian $H = H^{(1)} + H^{(2)}$ in a matrix formulation and diagonalize it numerically. By means of the diagonalization, we can find the eigenvalue E_i and the corresponding eigenstates $\psi_i(r,\theta,z)$ of equation (1). The eigenstates $\psi_i(r,\theta,z)$ will be used as basis functions afterwards.

Figure 1 shows the dependence of the electronic states on the orientation of the external magnetic field ($B = 17$ T). The four lowest states are presented with the structure parameters $H = 2$, $D = 7.5$ and $R = 12$ nm, the confining potential $V_0 = 1$ eV, corresponding to the band offset between InAs and GaAs, the effective mass $m_e = 0.023\ m_0$ for unstrained InAs, the effective mass $m_e = 0.067\ m_0$ for the GaAs barrier. The electronic states are mainly determined by $H^{(1)}$, while $H^{(2)}$ combines the states with $m' = m \pm 1$, and leads to anticrossing between these levels. When $\alpha = 0°$ (or 180°), the orientation of the magnetic field is perpendicular to the z direction. The Zeeman effect is zero; thus the levels L3 and L4 are degenerate separately. As the orientation of the magnetic field turns towards the z direction, the levels L3 and L4 split due to the Zeeman effect and the levels L1 and L2 get higher due to the effective potential $\Omega^2 R_y m_e \sin^2\alpha r^2/8\hbar$. As the magnetic field turns further to the z direction, the effective potential $\Omega^2 R_y m_e \sin^2\alpha r^2/8\hbar$ becomes more and more important, which can be understood easily from the fact that level L3 reverses the trend of getting lower. All crossings between levels are anticrossings due to $H^{(2)}$.

3. The electronic structures of two-electron quantum discs and two-electron quantum-disc qubits

In the following, we investigate the two-electron levels of vertically assembled quantum discs versus the orientation of the magnetic field. The spin-free Hamiltonian of the system can be expressed as

$$H = H_1 + H_2 + \frac{e^2}{\epsilon r_{12}}, \tag{8}$$

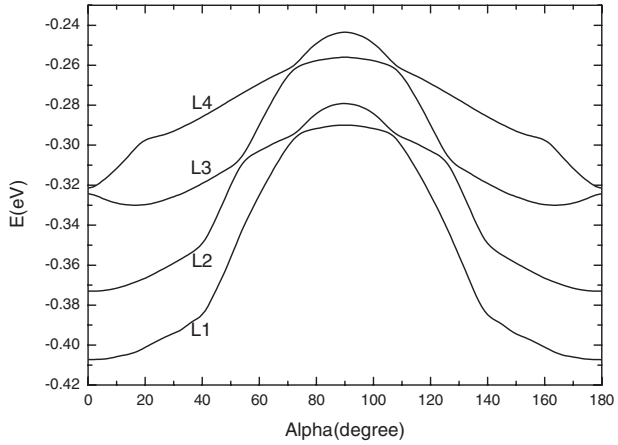

Figure 1. Four single-electron energies as functions of the orientation of the magnetic field ($B = 17$ T) with structure parameters $H = 2$ nm, $D = 7.5$ nm and $R = 12$ nm. Alpha is the polar angle relative to the y axis. Four levels are labelled L1, L2, L3 and L4.

where H_1 and H_2 are single-electron Hamiltonians of the system and we retain the formalism of equation (2). The Zeeman coupling $E_Z = g^*\mu_B B S_Z$ of the magnetic field to S_Z can be taken into account afterwards. We have obtained numerically the eigenstates $\psi(r, \theta, z)$ of the single-electron part of equation (8); thus the two-electron wavefunction with a total spin S can be expanded as [6]

$$\Psi_S(r_1, r_2) = \sum_{i \leqslant j} \alpha_{i,j}\{\psi_i(r_1, \theta_1, z_1)\psi_j(r_2, \theta_2, z_2) + (-1)^S \psi_i(r_2, \theta_2, z_2)\psi_j(r_1, \theta_1, z_1)\}, \qquad (9)$$

which is symmetric for $S = 0$ and antisymmetric for $S = 1$. Since the spin part of the wavefunction is not explicitly written, we will work with the spin-independent wavefunctions in the following. The coefficient vector $\boldsymbol{\alpha}_l$ and the corresponding energy E_l for the lth eigenstate are found from a generalized eigenvalue problem in which the Hamiltonian matrix elements can be calculated numerically. By changing the number of the basis functions, we can check the convergence and we find that it is sufficient for obtaining the two lowest double-electron states by using the four lowest single-electron states as the basis functions. This can be explained simply by the fact that the two double-electron states are mainly composed of the four single-electron states when the former states are expanded according to equation (9). Moreover, more double-electron states can be achieved by choosing more single-electron states as basis functions.

Figure 2 shows the dependence of the two lowest states on the orientation of the magnetic field ($B = 17$ T) in the range $\alpha = 0°$–$180°$, for the structure parameters $H = 2$ nm, $R = 12$ nm and $D = 7.5$ nm. The two lowest states possess different spins $S = 1$ and 0. When $\alpha = 0°$ ($180°$), the $S = 0$ state is lower than the $S = 1$ state. As the orientation of the magnetic field turns towards the z direction, the two lowest double-electron states approach each other. At $\alpha = 64°$–$72°$ and $108°$–$116°$, the $S = 1$ state becomes the lower one. We can explain the transition by means of the dependence of single-electron states on the magnetic field. The two double-electron states are composed mainly of two lowest single-electron states. As the magnetic field turns towards the z direction, the single-electron states approach each other. Similarly, the two lowest two-electron states will approach each other as the orientation of the magnetic field varies. If we do not take into account the electron interaction effects, the $S = 0$ state should remain lower forever, for the two electrons in the $S = 0$ state occupy

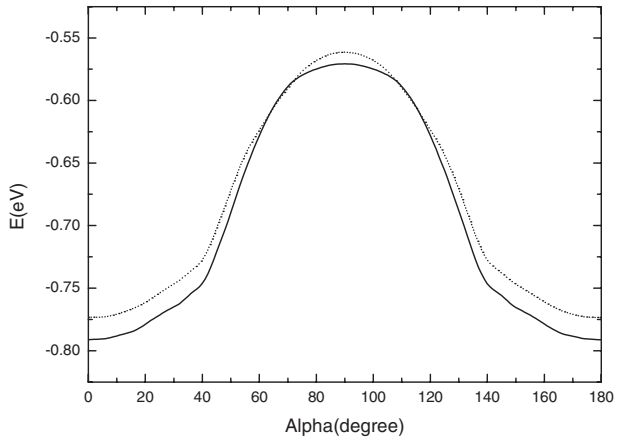

Figure 2. The two lowest two-electron states versus the orientation of the magnetic field ($B = 17$ T), for structure parameters $H = 2$ nm, $D = 7.5$ nm and $R = 12$ nm. Alpha is the polar angle relative to the y axis. The solid curve is for the $S = 0$ state and the dotted curve is for the $S = 1$ state.

the lowest single-electron state, while the two electrons in the $S = 1$ state cannot occupy the lowest single-electron state simultaneously according to the Pauli exclusion principle. Due to the effect of the electron interaction between the two electrons, the difference of the interaction energy between the two states makes the state $S = 1$ lower at some point, and thus a transition occurs. Now, we consider the effect of the Zeeman term on the energy levels. The energy of the $S = 1$ state is lowered by about 60 μeV T^{-1}, and that of the $S = 0$ state is unaltered. According to the order of magnitude of the energy levels, the Zeeman term can be neglected.

The energy difference ΔE between the lowest $S = 0$ and 1 states is plotted in figure 3, for structure parameters $H = 2$ nm, $R = 12$ nm and $D = 7.5$ nm. Since the ground state spin of the double-electron system is either $S = 0$ or 1, we can change the spin by adjusting the orientation of the magnetic field (see figure 3). The transition from the $S = 0$ to the 1 state allows us to use the total spin of the system as a qubit [6, 19] and an arbitrary single-qubit rotation can be generated by varying the orientation of the magnetic field. One can obtain the different regions of the $S = 0$ and 1 ground states by changing the structure parameters. At certain structure parameters, we can also obtain the different regions of the $S = 0$ and 1 ground states by changing the strength of the external magnetic field. In figure 4, we show the variation of the energy difference ΔE with the strength of the external magnetic field. With increasing strength of the external magnetic field, the two valleys of the $S = 1$ state become apart from each other and the peak of the $S = 0$ state becomes higher. The reason for this is that with increasing strength of the external magnetic field, its z direction component increases, which mainly determines the electronic structures. Moreover, since the typical size of the quantum disc is much smaller than that of the external confining potential in [6], the maximum energy difference ΔE in the $S = 1$ state is at least ten times as large as that in [6]. Since high-quality vertically stacked quantum discs can be fabricated successfully, it is realistic to envisage obtaining the qubit.

4. Conclusion

In conclusion, we have calculated the electronic structure of vertically assembled quantum discs as a function of the orientation of the applied magnetic field. The electronic structures are determined by the combined effect of the quantum confinement and the magnetic field.

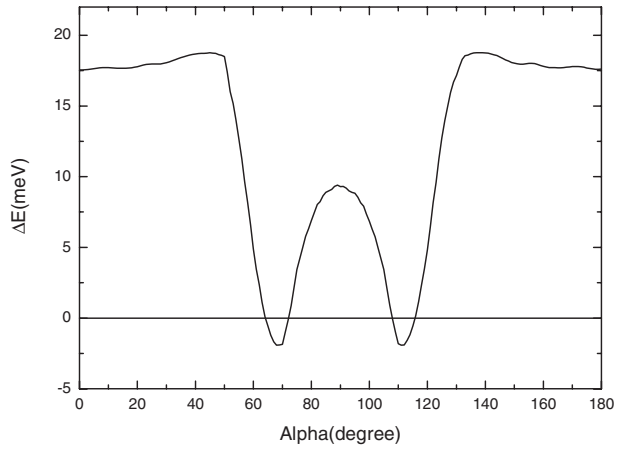

Figure 3. The energy difference between the triplet and singlet states ΔE as a function of the orientation of the magnetic field ($B = 17$ T), the structure parameters being the same as those in figure 2.

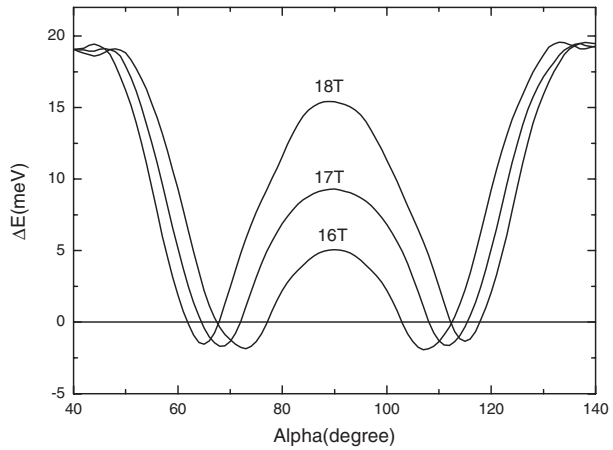

Figure 4. The energy difference between the triplet and singlet states ΔE as a function of the orientation of the magnetic field, with structure parameters $H = 2$ nm, $D = 7.5$ nm and $R = 12$ nm. The external magnetic field is given three different strengths ($B = 17$, 18, 19 T).

The change of the magnetic field as an effective potential strongly modifies the electronic structure, leading to splittings of levels and anticrossings between levels. The total spin of the two-electron ground state of the quantum-disc system can be changed by adjusting the orientation of the magnetic field. Our results support the possibility of using the system as a qubit [6] of a quantum computer. This kind of qubit is novel, as it can be controlled by the orientation of the magnetic field.

Acknowledgments

This work was supported by the National Natural Science Foundation of China (No 60025410, No 60176006) and the special Foundation for State Major Basic Research Programme of China (Grant No G2001CB309500).

References

[1] Kastner M A 1993 *Phys. Today* **46** (1) 24
[2] Palacios J J and Hawrylak P 1995 *Phys. Rev.* B **51** 1769
[3] Tokura Y, Austing D G and Tarucha S 1999 *J. Phys.: Condens. Matter* **11** 6023
Bryant G W 1993 *Phys. Rev.* B **47** 1683
[4] Pryor C 1998 *Phys. Rev. Lett.* **80** 3579
[5] Fonseca L R C, Jimenez J L and Leburton J P 1998 *Phys. Rev.* B **58** 9955
[6] Harju A, Siljamäki S and Nieminen R M 2002 *Phys. Rev. Lett.* **88** 226804
[7] Wasilewski Z R, Fafard S and McCaffrey J P 1999 *J. Cryst. Growth* **201** 1131
[8] Blick R H, Pfannkuche D, Haug R J, von Klitzing K and Eberl K 1998 *Phys. Rev. Lett.* **80** 4032
[9] Luyken R J, Lorke A, Fricke M, Kotthaus J P, Medeiros-Ribeiro G and Petroff P M 1999 *Nanotechnology* **10** 14
[10] Maximov M V *et al* 1998 *J. Appl. Phys.* **83** 5561
[11] Fafard S, Wasilewski Z R, Allen C N, Hinzer K, McCaffrey J P and Feng Y 1999 *Appl. Phys. Lett.* **75** 986
[12] Lundstrom T, Schoenfeld W, Lee H and Petroff P M 1999 *Science* **286** 2312
[13] Burkard G, Seelig G and Loss D 2000 *Phys. Rev.* B **62** 2581
[14] Pazy E *et al* 2003 *Europhys. Lett.* **62** 175
[15] Biolatti E *et al* 2002 *Phys. Rev.* B **65** 075306
[16] De Rinaldis S *et al* 2002 *Phys. Rev.* B **65** 081309
[17] Dong Q R, Li S S, Niu Z C, Feng S L and Zheng H Z 2004 *J. Appl. Phys.* **96** 3277
[18] Korkusinski M and Hawrylak P 2001 *Phys. Rev.* B **63** 195311
[19] Burkard G, Loss D and DiVincenzo D 1999 *Phys. Rev.* B **59** 2070